Journal of Applied Pharmaceutical Science Vol. 11(02), pp 029-038, February, 2021
Available online at http://www.japsonline.com
DOI: 10.7324/JAPS.2021.110204
ISSN 2231-3354

New benzothiazinone linked 1, 2, 4-triazoles: Design, synthesis, characterization, and evaluation of antitubercular activity

Kannampally Ajmal, Gurubasavaraj V. Pujar*, Sethu Arun Kumar, Subhankar P. Mandal, Manisha Singh
Department of Pharmaceutical Chemistry, JSS College of Pharmacy, JSS Academy of Higher Education and Research, Mysuru 570 015 India.

ARTICLE INFO

Received on: 07/08/2020
Accepted on: 28/12/2020
Available online: 05/02/2021

Key words:
1, 2, 4-triazole, benzo[1,4] thiazin-3(4H)-one, MABA, *Mycobacterium tuberculosis*, MTT assay, DprE1 inhibitors.

ABSTRACT

Introduction: In a quest for developing active molecules to treat tuberculosis, we reported the design, synthesis, and antitubercular activity evaluation of benzo[1, 4]thiazin-3(4H)-one encompassed 1, 2, 4-triazoles targeting the DprE1 (Decaprenylphosphoryl-beta-D-ribose oxidase) enzyme involved in cell wall component biosynthesis.

Methodology: The antitubercular potential of the title compounds was screened against the standard strain of *Mycobacterium tuberculosis* H37Rv by Microplate Alamar Blue Assay (MABA) and in vitro cytotoxicity was screened against in human embryonic kidney 293 (HEK293T) cells. The prediction of ligand interactions to the target DprE1 enzyme's binding site was realized through a molecular docking study.

Results: Synthesized molecules have shown good antitubercular activity with reference to the standard antitubercular drugs. The **5c**, **5e**, and **6c** are the most active antitubercular compounds having a minimum inhibitory concentration of 12.5 µg/ml. The synthesized molecules' cytotoxic data reveal that tested compounds exhibited low *in vitro* cytotoxicity (higher IC_{50} values) in human embryonic kidney 293 (HEK293T) cells. Moreover, the prediction of ligand interactions to the target DprE1 enzyme's binding site was realized through a molecular docking study. The compounds **6a–d** have shown good docking scores, and their interactions with amino acids with active site pockets of the DprE1 were in line with the reference ligand.

Conclusion: Thus, the adopted docking protocol is in good correlation to the *in vitro* antitubercular activity. Hence, benzo[1, 4]thiazin-3(4H)-one encompassed 1, 2, 4-triazole scaffolds may provide the basis for developing new DprE1 inhibitors.

INTRODUCTION

Tuberculosis (TB) is continuing to affect humankind with broad population statistics. It reached approximately 1.9 million deaths and is increasing in number every year (Rojano *et al*., 2019). The recent emergence of the disease with multidrug-resistant tuberculosis, total drug resistance, and extensively drug-resistant TB strains (Prasad *et al*., 2017) has increased the mortality rate by several folds, which in turn prompts the necessity for the discovery of drug which can reduce the load of the resistant strains of TB (Akkerman *et al*., 2019). Recently, several antitubercular drugs were in the drug discovery pipeline, and few were in the developmental stage (Libardo *et al*., 2018). However, due to enormous cases of failure in the early stage of drug development, there is a constant need for novel drug candidates with possibly novel scaffold possessing efficacy to combat all kinds of resistant TB cases.

Mycobacterium tuberculosis (Mtb) owns an elegant cell wall due to the presence of arabinogalactan and mycolic acid along with the peptidoglycan layer, which is reversibly connected to the outer layer of protein and polysaccharide (Abrahams and Besra, 2018). The well-known first-line anti-TB drug isoniazid (INH) inhibits a vital enzyme involved in mycolic acid biosynthesis, and ethambutol targets the enzymes involved in arabinan biosynthesis. Likewise, few among the best active antibiotics in contrast to TB act by suppressing the cell wall synthesis (Wolucka *et al*., 1994). Validation of the new target DprE1, a key enzyme in producing an intermediate decaprenyl-phospho-arabinose (DPA) in cell wall components' biosynthesis, has emerged as a promising target in developing antitubercular agents (Brecik *et al*.,

*Corresponding Author
Gurubasavaraj V. Pujar, Department of Pharmaceutical Chemistry, JSS College of Pharmacy, JSS Academy of Higher Education and Research, Mysuru, India. E-mail: gvpujar @ jssuni.edu.in

2015). DprE1 is a vital Mtb flavoenzyme encoded by the dprE1 gene (*rv3790*) named decaprenophosphoryl-beta-D-ribose-2-oxidase (Makarov *et al*., 2009). DprE1 works in harmony with the DprE2 (Decaprenylphosphoryl-2-keto-beta-D-erythro-pentose reductase) enzyme that helps in the epimerization of decaprenyl-phosphoribose (DPR) to DPA. DprE1 utilizes FAD (Flavin Adenine Dinucleotide) to oxidate DPR to a ketonic derivative and later undergoes reduction to DPA, an exclusive precursor in the synthesis of lipopolysaccharides (lipoarabinomannan and arabinogalactan) by NADH (reduced Nicotinamide Adenine Dinucleotide) dependent DprE2. Both DprE1 and DprE2 are indispensable for cell growing and Mtb's existence (Brecik *et al*., 2015). Benzothiazinones (BTZ) (Batt *et al*., 2012), dinitrobenzamides (Li *et al*., 2018), nitroimidazoles (Kim *et al*., 2009), and nitroquinoxalines (Magnet *et al*., 2010) with chemically diverse molecules were found to be active as covalent DprE1 inhibitors. They displayed significant antitubercular activity in both *in vitro* and *in vivo* efficacy studies. Few studies have shown that the replacement of the nitro group on BTZ by the azide group or pyrrole ring also offered substantial antitubercular activity, while their mode of inhibition changed from a covalent to non-covalent fashion (Tiwari *et al*., 2016; Zhang *et al*., 2014). As a result of cell-based screening, TCA1 (a benzothiazole derivative) demonstrated potency against non-replicating and replicating Mtb was identified with an effective *in vivo* activity alone or combined with the first-line drugs (Wang *et al*., 2013). Keeping TCA1 as a lead, a structure-based drug discovery approach had witnessed the report of several non-covalent DprE1 inhibitors in the last few years (Makarov *et al*., 2015; Manina *et al*., 2010; Naik *et al*., 2014; Shirude *et al*., 2013; Tiwari *et al*., 2016; Wang *et al*., 2013).

Triazole (1, 2, 3-triazole/1, 2, 4-triazole) moiety is a critical five-membered heterocycle, an integral moiety in various clinically approved drugs (Maddila *et al*., 2013). It has been explored to synthesize new molecules with varied infection-related activities (Keri *et al*., 2015). Several studies have revealed the promising effect of triazole as antitubercular agents (Bangalore *et al*., 2019; Karabanovich *et al*., 2019; Reddyrajula *et al*., 2020; Shaikh *et al*., 2019; Zampieri *et al*., 2019). Furthermore, the conjunction of 1, 2, 4-triazole with other azoles (heterocyclic systems) has resulted in potential antitubercular activity against DprE1 target (Karabanovich *et al*., 2019; Shaikh *et al*., 2016, 2019), including our earlier work on exploring the antitubercular potential of triazoles (Krishna *et al*., 2014; Neenu *et al*., 2020). The strategy for the design of title compounds (Fig. 1) was based on the antitubercular potentials of two heterocyclic ring systems, benzo[1, 4]thiazin-3(4*H*)-one and 1, 2, 4-triazole. The introduction of aryl/cycloalkyl groups (R) at the fourth position of triazole and the nitro benzoyl group at thiol of triazoles increases the lipophilicity of the prefinal and final compounds (Arnott *et al*., 2012; Shaikh *et al*., 2016). Furthermore, the introduction of nitro benzoyl functionality realizes antitubercular potentials. Based on these findings, an effort is conceived to explore the *in vitro* efficacy of benzothiazinone conjugate of 1,2,4-triazoles against Mtb.

MATERIALS AND METHODS

Solvents and chemicals were procured from Sigma-Aldrich, TCI chemicals and were utilized as received to prepare intermediates and final compounds. The synthesized compounds' melting point was determined using the one-end open capillary tube method using a digital melting point apparatus. The reaction's progress was determined on thin-layer chromatography (TLC) using aluminum plates (Merck) with silica gel 60 F254. Infrared (IR) spectra were recorded using Shimadzu FT-IR (Fourier Transform-Infrared spectroscopy). ^{13}C and $^{1}HNMR$ spectra were recorded using a Bruker AMX-300 NMR spectrometer at 400 MHz. Chemical shifts (δ) were reported in parts per million (ppm) using tetramethylsilane as the reference. Mass spectra were recorded on liquid chromatography–mass spectrometry (LCMS) from Agilent technologies in Electrospray ionization mode. Elemental analysis was conducted for the synthesized compounds, and the values obtained were within 0.3% of the calculated values.

Synthesis of 2H-benzo[b][1, 4]thiazin-3(H)-one (1)

Equimolar quantities (0.04 mol) of 2-amino thiophenol and chloroacetic acid were taken in a 150 ml round bottom flask (RBF) and glacial acetic acid (40 ml) and sodium acetate (equimolar) were added. The reaction content was heated at a boiling temperature for 24 hours. The reaction's progress was

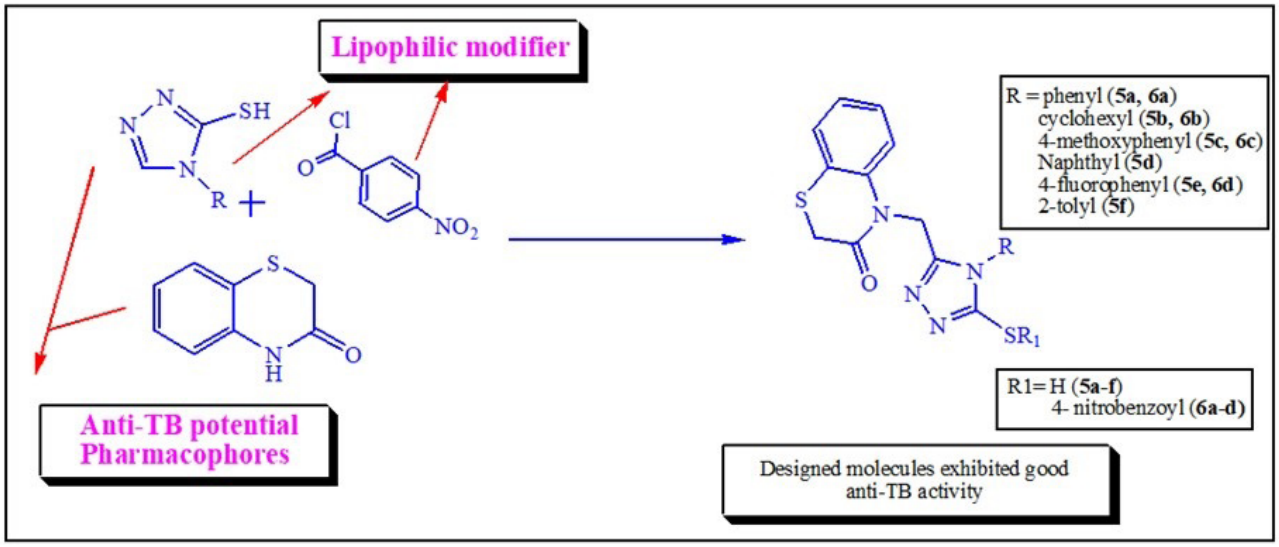

Figure 1. Design strategy for the proposed compounds.

checked by TLC using hexane and ethyl acetate as mobile phase (1:2). Then, the final content was poured into ice cold water. The solids were separated by filtration, and then dried and recrystallized using 70% ethanol.

Yield: (5.2 g, 78%). mp: 179°C–181°C (Literature value:176°C–178°C); IR (KBr) cm^{-1}: 3,024 (Ar C-H), 3,359 (N-H), 1,702 (C=O); ^{1}H NMR dimethyl sulfoxide (DMSO-*d6*, δ ppm): 3.42 (s, 2H, CH_2), 6.80–7.31 (m, 4H, Ar H:), 8.61 (s, 1H, NH); ^{13}C NMR (DMSO-*d6*, *δ* ppm): 40.6 (CH_2), 123.5, 124.6, 125.8, 130.0, 136.0, 143.1 (C-N), 166.88 (C=O); LCMS: 165.02 [M^+].

Synthesis of ethyl 2-(2, 3-dihydro-3-oxobenzo[b][1, 4]thiazin-4-yl)acetate (2)

An equimolar quantity of 2*H*-benzo[b][1,4]thiazin-3(4*H*)one (0.04 mol) and ethyl bromoacetate (0.04 mol) were transferred to dry acetone (15 ml) in the presence of anhydrous potassium carbonate (0.04 mol). The reaction content was heated to a refluxing temperature for 22 hours. The progress of the reaction was observed by TLC using mobile phase hexane and ethyl acetate in the ratio of 1:2 and once the reaction was completed, it was filtered off the potassium carbonate. The filtrate acetone was removed using a rotary vacuum evaporator to get the desired product (**2**).

Yield: (4.52 g, 67%). mp: (ND); IR (KBr) cm^{-1}: 3,026 (Ar C-H), 1,654 and 1,702 (C=O); ^{1}H NMR (DMSO-*d6*, δ ppm): 1.46 (t, 2H, CH_3), 3.52 (s, 2H, CH_2), 4.23 (m, 2H, CH_2), 4.43 (s, 2H, CH_2), 6.92–7.30 (m, 4H, ArH),^{13}C NMR (DMSO-*d6*, *δ* ppm):15.3 (CH_3), 40.6 (CH_2), 51.0 (CH_2), 61.4 (CH_2), 123.5, 124.1, 125.1, 130.0, 133.0, 138.1 (C-N), 166.23 (C=O); LCMS *m/z*: 251.03 [M^+].

Synthesis of 2-(2, 3-dihydro-3-oxobenzo[b][1, 4]thiazin-4yl) acetohydrazide (3)

Ethyl 2-(2,3-dihydro-3-oxobenzo[b][1, 4] thiazin-4yl) acetate (0.01 mol) was taken in an RBF and dissolved in ethanol (10 ml). To this, 99% hydrazine hydrate (0.01 mol) was added dropwise and the reaction mixture was stirring overnight at room temperature. The progress of the reaction was observed by TLC using chloroform and methanol as a mobile phase (4:1). The solid separated was filtered, dried, and recrystallized using ethanol.

Yield: (6.73 g, 71%). mp: 186°C–189°C; IR (KBr) ν cm^{-1}: 3,365 and 3,630 (N-H), 3,021 (Ar C-H), 1,654 and 1,765 (C=O); ^{1}H NMR (DMSO-*d6*, δ ppm): 3.52 (s, 2H, CH_2), 4.43 (s, 2H, CH_2), 7.1–7.3 (m, 4H, ArH), 9.63 (bs, 2H, NH), 10.30 (s, 1H, NH), ^{13}C NMR (DMSO-*d6*, *δ* ppm): 41.1 (CH_2), 52.0 (CH_2), 123.5, 124.1, 125.1, 131.1, 133.3, 138.5 (C-N), 167.27 (C=O); LCMS *m/z*: 237.06 [M^+].

Synthesis of 4-((5-mercapto-4-aryl/cyclohexyl-4H-1, 2, 4-triazol-3-yl)methyl)-2H-benzo[b][1,4]thiazin-3(4H)-ones (5a–5f)

An equimolar quantity (0.004 mol) of acetohydrazide derivative (**3**) and different aryl/cyclohexyl isothiocyanates were dissolved in solvent ethanol, and the reaction content was refluxed for 3–8 hours. The white solids were obtained on cooling the reaction content, then filtered and dried to obtain carbothioamide derivatives (**4a–4f**). The product formed was directly used for the subsequent reaction step. Compound **4a** (0.004 mol) was taken in an RBF and dissolved in 2 M NaOH solution (12 ml) and refluxed to a boiling temperature for 8 hours. TLC monitored the completion of the reaction. The mixture was then cooled and filtered. Upon acidification of filtrate using 2 M HCl, the product precipitated out. The obtained precipitate was filtered, washed with water, dried, and recrystallized from absolute alcohol.

4-((5-mercapto-4-phenyl-4H-1, 2, 4-triazol-3-yl)methyl)-2H-benzo[b][1,4]thiazin-3(4H)-one (5a)

Yield: (0.90 g, 64%). mp: 210°C–216°C; IR (KBr) cm^{-1}: 3,294 (N-H), 3,009 (Ar C-H), 1,724 (C=O), 1,585 (C=S); ^{1}H NMR (DMSO-*d6*, δ ppm): 3.41 (s, 2H, CH_2), 4.23 (s, 2H, CH_2), 6.53–7.55 (m, 9H, ArH), 13.78(s, 1H, NH); ^{13}C NMR (DMSO-*d6*, δ ppm): 38.9, 56.0, 124.5, 125.2, 125.3, 128.4, 129.0, 133.0, 133.9, 135.0, 135.7, 157.0, 166.7; LCMS *m/z*: 355.07 (M^+); Anal. Calcd. for $C_{17}H_{14}N_4OS_2$: C, 57.61; H, 3.98; N, 15.81; O, 4.51; S, 18.09, found: C, 56.4; H, 3.66; N, 15.17.

4-((4-cyclohexyl-5-mercapto-4H-1,2,4-triazol-3-yl)methyl)-2H-benzo[b][1,4]thiazin-3(4H)-one (5b)

Yield: (0.96 g, 67%). mp: 196°C–202°C; IR (KBr) cm^{-1}: 3,340 (N-H), 2,852 (Aliphatic C-H), 1,724 (C=O), 1,585 (C=S); ^{1}H NMR (DMSO-*d6*, δ ppm): 1.15–2.93 (m, 11H, cyclohexyl), 3.29 (s, 2H, CH_2), 4.49 (s, 2H, CH_2), 6.51–7.31 (m, 4H, ArH), 13.52 (s, 1H, NH); ^{13}C NMR (DMSO-*d6*, δ ppm): 24.7, 25.7, 32.8, 39.2, 49.1, 56.5, 124.5, 125.2, 135, 135.7, 155.6, 162.3, 166.7; LCMS *m/z*: 361.4 (M^+); Anal. calcd. for $C_{17}H_{20}N_4OS_2$: C, 56.23; H, 5.59; N, 15.54; O, 4.44; S, 16.68, found: C, 56.14; H, 5.11; N, 16.01.

4-((5-mercapto-4-(4-methoxyphenyl)-4H-1, 2, 4-triazol-3-yl) methyl)-2H-benzo[b][1, 4]thiazin-3(4H)-one (5c)

Yield:(0.95 g, 62%). mp: 234°C–238°C; IR (KBr) cm^{-1}: 3,581 (N-H), 3,024 (Ar C-H), 1,716 (C=O), 1,591 (C=S); ^{1}H NMR (DMSO-*d6*, δ ppm): 3.40 (s, 2H, CH_2), 3.78 (s, 3H, CH_3), 4.43 (s, 2H, CH_2), 6.43–7.35 (m, 8H, ArH), 13.52 (s, 1H, NH); ^{13}C NMR (DMSO-*d6*, δ ppm): 38.9, 55.8, 56.0, 114.6, 124.5, 125.2, 134.8, 135.7, 137.8, 151.6, 160.6, 166.7, 168.9; LCMS *m/z*: 385.84 (M^+); Anal. calcd. for $C_{18}H_{10}N_4O_2S_2$: C, 56.23; H, 4.19; N, 14.57; O, 8.32; S, 16.68, found: C, 56.33; H, 4.27; N, 13.88.

4-((5-mercapto-4-(naphthalen-1-yl)-4H-1,2,4-triazol-3-yl) methyl)-2H-benzo[b][1,4]thiazin-3(4H)-one (5d)

Yield: (1.14 g, 71%). mp: 212°C–216°C; IR (KBr) cm^{-1}: 3,358 (N-H), 3,053 (Ar C-H), 1,708 (C=O), 1,589 (C=S); ^{1}H NMR (DMSO-*d6*, δ ppm): 3.43 (s, 2H, CH_2), 4.05 (s, 2H, CH_2), 6.33–7.66 (m, 11H, ArH), 13.82 (s, 1H, NH); ^{13}C NMR (DMSO-*d6*, δ ppm): 39.2, 48.2, 123.9, 124.5, 125.2, 125.3, 126.3, 126.7, 128.3, 131.6, 133.7, 135.0, 135.7, 138.2, 151.6, 166.7, 168.9; LCMS *m/z*: 404.7 (M^+); Anal. calcd. for $C_{21}H_{16}N_4OS_2$: C, 62.36; H, 3.99; N, 13.85; O, 3.96; S, 15.85, found: C, 61.97; H, 4.11; N, 13.71.

4-((4-(4-fluorophenyl)-5-mercapto-4H-1,2,4-triazol-3-yl) methyl)-2H-benzo[b][1,4]thiazin-3(4H)-one (5e)

Yield: (0.99 g, 67%). mp: 198°C–202°C; IR (KBr) cm^{-1}: 3,320 (N-H), 3,119 (Ar C-H), 1,731 (C=O), 1,587 (C=S); ^{1}H NMR (DMSO-*d6*, δ ppm): 3.64 (s, 2H, CH_2), 4.15 (s, 2H, CH_2), 6.41–7.45 (m, 9H, ArH), 13.52 (s, 1H, NH); ^{13}C NMR (DMSO-*d6*, δ ppm): 39.2, 48.2, 115.5, 124.5, 125.2, 130.1, 135.0, 135.7, 141.1,

151.6, 162.9, 166.7, 168.9; LCMS *m/z*: 372.1 (M^+); Anal. calcd. for $C_{17}H_{13}FN_4OS_2$: C, 54.82; H, 3.52; F, 5.10; N, 15.04; O, 4.30; S, 17.22, found: C, 55.11; H, 3.54; N, 15.17.

4-((5-mercapto-4-(p-tolyl)-4H-1,2,4-triazol-3-yl)methyl)-2H-benzo[b][1,4]thiazin-3(4H)-one (5f)

Yield: (0.92 g, 63%). mp: 220°C–226°C; IR (KBr) cm^{-1}: 3,298 (N-H), 3,047 (Ar C-H), 1,754 (C=O), 1,589 (C=S); ^{1}H NMR (DMSO-*d6*, δ ppm): 2.25 (s, 3H, CH_3), 3.37 (s, 2H, CH_2), 4.50 (s, 2H, CH_2), 6.52–7.31 (m, 8H, ArH), 13.48 (s, 1H, NH); ^{13}C NMR (DMSO-*d6*, δ ppm): 21.3, 39.2, 48.4, 124.5, 125.2, 129.0, 131.0, 135, 135.7, 138.4, 142.5, 151.6, 166.7, 168.9; LCMS *m/z*: 368.3 (M^+); Anal. calcd. for $C_{18}H_{16}N_4OS_2$: C, 58.67; H, 4.38; N, 15.21; O, 4.34; S, 17.40.

Synthesis of S-(5-((3-oxo-2,3-dihydro-4H-benzo[b][1,4] thiazin-4-yl)methyl)-4-aryl/alkyl-4H-1,2,4-triazol-3-yl) 4-nitrobenzothioates (6a–d)

An equimolar quantity (0.002 M mol) of 4-nitrobenzoyl chloride and appropriate 1,2,4-triazoles (**5a–c, 5e)** were added to dry acetone in the presence of Cs_2CO_3 (0.002 M mol), and the reaction content was refluxed for 14 hours. The reaction progress was observed by TLC using chloroform and methanol as a mobile phase (3:1). Once the reaction was completed, the reaction mixture was filtered, and the collected filtrate was evaporated using rotary vacuum evaporator to get the desired compound.

S-(5-((3-oxo-2,3-dihydro-4H-benzo[b][1, 4]thiazin-4-yl) methyl)-4-phenyl-4H-1,2,4-triazol-3-yl) 4-nitrobenzothioate (6a)

Yield: (0.76 g, 76%). mp: 236°C–240°C; IR (KBr) cm^{-1}: 3,298 (N-H), 3,024 (Ar C-H), 1,708, 1,724 (C=O), 1,606 (C=S), 1,501(N-O); ^{1}H NMR (DMSO-*d6*, δ ppm): 3.42 (s, 2H, CH_2), 4.23 (s, 2H, CH_2), 6.91–8.03 (m, 9H, ArH), 8.26–8.38 (m, 4H, ArH); ^{13}C NMR (DMSO-*d6*, δ ppm): 39.3, 49.1, 124.1, 124.5, 129.0, 129.6, 135.0, 135.7, 140.8, 145.5, 151.6, 153.3, 159.7, 166.7, 187.6, 187.7; LCMS *m/z*: 504.43 (M^+); Anal. Calcd. for $C_{24}H_{17}N_5O_4S_2$: C, 57.25; H, 3.40; N, 13.91; O, 12.71; S, 12.73, found: C, 56.84; H, 3.46; N, 13.27.

S-(4-cyclohexyl-5-((3-oxo-2,3-dihydro-4H-benzo[b] [1,4]thiazin-4-yl)methyl)-4H-1,2,4-triazol-3-yl) 4-nitrobenzothioate (6b)

Yield: (074 g, 73%). mp: 228°C–232°C; IR (KBr) cm^{-1}: 3,140 (Ar C-H), 1,718, 1,729 (C=O), 1,599 (C=S), 1,475 (N-O); ^{1}H NMR (DMSO-*d6*, δ ppm): 1.15–2.93 (m, ^{11}H, cyclohexyl), 3.30 (s, 2H, CH_2), 4.49 (s, 2H, CH_2), 6.89–8.01 (m, 4H, ArH), 8.26–8.32 (m, 4H, ArH); ^{13}C NMR (DMSO-*d6*, δ ppm): 24.7, 25.7, 33.2, 39.5, 39.3, 49.1, 57.1, 124.1, 124.5, 129.0, 129.6, 135.0, 135.7, 140.8, 145.5, 151.6, 153.3, 159.7, 166.7, 187.6, 187.7; LCMS *m/z*: 510.78 (M^+); Anal. calcd. for $C_{24}H_{23}N_5O_4S_2$: C, 56.57; H, 4.55; N, 13.74; O, 12.56; S, 12.58, found: C, 57.01: H, 4.54; N, 13.11.

S-(4-(4-methoxyphenyl)-5-((3-oxo-2,3-dihydro-4H-benzo[b][1,4]thiazin-4-yl)methyl)-4H-1,2,4-triazol-3-yl) 4-nitrobenzothioate (6c)

Yield: (0.72 g, 68%). mp: 216°C–220°C; IR (KBr) cm^{-1}: 3,162 (Ar C-H), 1,713, 1,739 (C=O), 1,579 (C=S), 1,535 (N-O); ^{1}H NMR (DMSO-*d6*, δ ppm): 3.40 (s, 2H, CH_2), 3.78 (s, 3H, CH_3), 4.42 (s, 2H, CH_2), 6.72–8.03 (m, 8H, ArH), 8.22–8.30 (m, 4H, ArH); ^{13}C NMR (DMSO-*d6*, δ ppm): 39.3, 49.1, 56.1, 114.3, 124.1, 124.5, 129.0, 129.6, 134.8, 135.0, 140.8, 145.5, 151.6, 153.3, 159.7, 166.7, 187.6, 187.7; LCMS *m/z*: 533.0 (M^+); Anal. calcd. for $C_{25}H_{19}N_5O_5S_2$: C, 56.28; H, 3.59; N, 13.13; O, 14.99; S, 12.02, found: C, 57.01: H, 3.44; N, 12.93.

S-(4-(4-fluorophenyl)-5-((3-oxo-2,3-dihydro-4H-benzo[b][1,4]thiazin-4-yl)methyl)-4H-1,2,4-triazol-3-yl) 4-nitrobenzothioate (6d)

Yield: (0.66 g, 64%). mp: 231°C–235°C; IR (KBr) cm^{-1}: 3,103 (Ar C-H), 1,699, 1,731 (C=O), 1,563 (C=S), 1,526 (N-O); ^{1}H NMR (DMSO-*d6*, δ ppm): 3.40 (s, 2H, CH_2), 4.42 (s, 2H, CH_2), 6.79–8.01(m, 8H, ArH), 8.20–8.33 (m, 4H, ArH); ^{13}C NMR (DMSO-*d6*, δ ppm): 39.2, 48.8, 115.5, 124.1, 124.5, 129.0, 130.1, 135.0, 135.7, 140.8, 141.1, 151.6, 153.3, 159.7, 162.7, 166.7, 187.6; LCMS *m/z*: 521.5 (M^+); Anal. calcd. for C_{24} $H_{16}FN_5O_4S_2$: C, 55.27; H, 3.09; F, 3.64; N, 13.43; O, 12.27; S, 12.29, found: C, 55.31; H, 2.94; N, 13.32.

***In vitro* antitubercular activity**

In vitro antitubercular activity of the synthesized molecules was tested by the MABA method (Coxon *et al*., 2012; Leonard *et al*., 2008) against *M. tuberculosis* H37Rv strain (ATCC 27294). *Mtb* suspension stock culture from Middlebrook 7H9-S was vortexed and adjusted to 1 McFarland standard (3 ×108 CFU/ml (Colony Forming Unit/ml)). The culture was further diluted to 2×10^5 CFU/ml concentration and used as inoculum. Test samples and standard drug stock solutions of 20,000 µg/ml concentration was prepared with DMSO. Serially the stock solutions (4×) were diluted using media into a 96-well plate to achieve working solutions. Twofold serial dilutions of the test compounds were prepared on the well plate, and 100 µl of inoculum (2 × 105 CFU/ml) and 100 µl media were added to each well of the 96-well plate to obtain a concentration of 200 µl. The final concentrations of test compounds and standard drugs (pyrazinamide, ciprofloxacin, and streptomycin) were between 0.8 and 100 µg/ml. Positive control (inoculum), DMSO as a blank, and negative control (media) in the plate were used to lessen the error. Then, the plates under aeration were incubated at 37°C. alamarBlue reagent (20 µl) was added on day 7 of incubation to each well plate and further incubated for 24 hours at 37°C. The color of the media changing from blue to pink was considered as the Mycobacterium's growth at a particular drug concentration. The test compound's well plate color matched with the color of the growth control well plate to understand the results better. The lowest drug concentration that inhibited bacterial growth was referred to as minimum inhibitory concentration (MIC).

***In vitro* cytotoxicity (CC_{50})**

The synthesized molecules were assessed for *in vitro* CC_{50} by 3-(4,5-Dimethylthiazol-2-yl)-2,5-diphenyltetrazolium bromide (MTT assay) (Chang *et al*., 2010) involving human embryonic kidney 293 cells (HEK293T). The test compound's 300–25 µg/ml concentrations were prepared in the 96-well plate containing the minimum essential medium without the fetal bovine serum. The well plate was then upturned onto a filter paper so that the resilient media could be separated and washed with PBS (Phosphate

Buffered Saline) gently. The outer perimeter walls were treated with 100 µL of sterile water. Then, the prepared dilutions were added (100 µl) into the wells. The plates were incubated with 5% CO_2 considering 72 hours for HEK293T cells at 37°C. This was succeeded by supernatant media removal by following the procedure mentioned earlier, and then it was washed with PBS. The MTT solution (50 µl) was supplemented to each well in a place devoid of light and was again subjected to incubation for 3 hours. The MTT solution was removed by inversion method, and DMSO was poured into every well and was placed aside in the dark for nearly 1–2 hours. ELISA (Enzyme-linked Immunosorbent Assay) reader was employed to record the optical density readings using a wavelength of 540 nm. CC_{50} was determined by deducing a graph obtained by taking test compound concentration and % of cell inhibition on the x-axis and y-axis, respectively.

$$\% \text{ Cytotoxicity} = \frac{\text{Control Absorbance} - \text{Test Absorbance}}{\text{Control absorbance}} \times 100$$

In silico absorption, distribution, metabolism, elimination, and toxicity (ADMET) prediction

Pharmacokinetic properties such as ADMET of compound structures were checked using the ADMETSAR web server and the Discover Studio 19.0 software package. Molecules were prepared accordingly via ligand preparation tools and subjected to ADMET predictions. The lipophilicity (clogP) of the compounds was predicted using Chemdraw software.

Molecular docking study

Docking study is like a lock and key concept, executable by implementing various algorithms (Inturi *et al*., 2016). LIBDOCK algorithm was implemented in the present study by CHARMm force field (Biovia Discovery Studio 19.0 software). The preamble to docking procedure, protein's 3D structure (PDB ID-4PFD) was downloaded from the Protein databank (PDB) (http://www.rcsb.org). The x-ray crystallographic form of DprE1 with a resolution of 2.30 Å was used to execute a protein preparation protocol to correct the side chains and loops region, followed by energy minimization. Consecutively, the water molecules and co-crystallized ligand were removed. Then, ligands were subjected further for duplicate removal and to fix their chemical valences. So, the prepared DprE1 protein and ligands were taken for the docking protocol. The binding site within the protein was recognized "from the receptor cavity" tool site search by means of flood-filling algorithm. Among other designated sites, the prime site 1 was found to be a potential one with a volume of 1,231 Å and a point count of 7,824 in equal grid spacing of 0.5 in three coordinate axes. The designed ligands and reference molecule were subjected to docking by default simulation annealing and fast conformation generation with a high precision mode that generates random conformations with 1,000 steps of dynamics. The top pose results were taken for the interactions study.

RESULTS AND DISCUSSION

Chemistry

The synthesis of intermediates and final compound structures was achieved as per the structure shown in Scheme 1. 2-aminothiophenol was reacted with 2-chloroacetic acid in the presence of sodium acetate to obtain 2H-benzo[b][1, 4] thiazin-3(4*H*)-one (**1**) (Shaikh *et al*., 2016; Rajender *et al*., 2019). N-alkylation of compound **1** was achieved through ethyl bromoacetate to offer ethyl 4-(benzo[1,4]thiazin-3-one)acetate (**2**). The 4-(benzo[1,4]thiazin-3-one) acetohydrazide (**3**) (Krishna *et al*., 2014) was prepared by a reaction between compound **2** and hydrazine hydrate in ethanol at an ambient temperature on overnight stirring. The reaction of acetohydrazide (**3**) with different alkyl/aryl isothiocyanates yields 4-(benzo[1,4]thiazin-3-one)carbothioamides (**4a–f**). The 4-((4-aryl/cycloalkyl-5-thioxo-4,5-dihydro-1*H*-1,2,4-triazol-3-yl)methyl)-2*H*-benzo[b][1,4] thiazin-3(4*H*)-ones (**5a–f**) were conveniently synthesized from

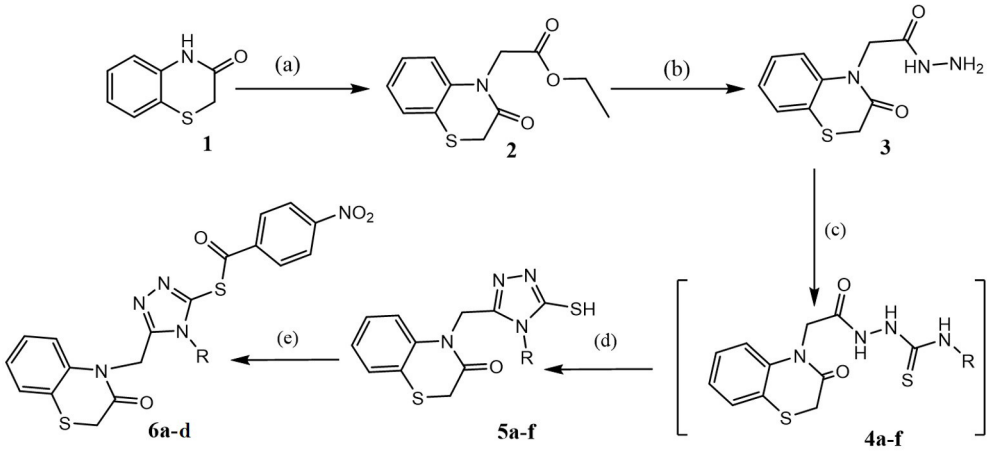

R = phenyl (5a, 6a), cyclohexy (5b, 6b), 4-methoxyphenyl (5c, 6c), naphthyl (5d), 4-fluorophenyl (5e, 6d) , 2-tolyl (5f)

Reagents and condition: a) $BrCH_2COOC_2H_5$, dry K_2CO_3 acetone, reflux b) $NH_2NH_2.H_2O$, C_2H_5OH, stirring c) RNCS, C_2H_5OH, reflux d) 2N NaOH reflux, neutralize with 2N HCl, e) *p*-NO_2 C_6H_4COCl, Cs_2CO_3 in dry acetone.

Scheme 1. Synthesis of benzothiazinone linked 1,2,4-triazoles.

carbothioamides (**4a–f**) by reflexing under the strong alkaline (2N NaOH) condition, followed by acidification with 2N HCl (Karabanovich *et al*., 2019). The target compounds, S-(5-((3-oxo-2,3-dihydro-4*H*-benzo[b][1,4]thiazin-4-yl)methyl)-4-aryl/alkyl-4*H*-1,2,4-triazol-3-yl) 4-nitrobenzothioates (Rabie *et al*., 2017) (**6a–d**) were synthesized by S-alkylation of appropriate compounds (**5a–c** and **5e**) with 4-nitrobenzoyl chloride in a solvent of dry acetone and cesium carbonate (Cs_2CO_3). All the intermediates and final compounds were synthesized in good yield (69%–75%). The reaction's progress was checked by TLC through an appropriate solvent system in each reaction step. The compounds' structures were characterized by a spectral study and are consistent with the proposed structures for intermediates and final compounds.

The IR spectrum of 2*H*-benzo[b][1, 4]thiazin-3(4*H*)-one (1) exhibits a characteristic peak at 3,359 cm^{-1} for NH, 1,702 cm^{-1} for C=O, and at 3,024 cm^{-1} for aromatic C-H group. The ^{1}H NMR spectrum of compound **1** integrates for seven protons. The multiplet peaks at 6.80–7.31 ppm integrate for aromatic protons, a singlet at 8.61 ppm for the proton of NH, and a singlet at 3.42 ppm for the CH_2 protons of benzothiazinone indicates that compound **1** was formed. The IR spectral analysis of compound **2** exhibits two characteristic carbonyl peaks in the regions of 1,654, 1,702, and 3,026 cm^{-1} for the aromatic C-H group. The ^{1}H NMR spectrum of compound **2** integrates for 13 protons. The multiplet at 6.92–7.30 ppm integrates for aromatic protons. A triplet resonates at 1.46 ppm for CH_3 protons of ester. A multiplet of OCH_2 protons at 4.23 ppm and a singlet at 4.43 ppm for CH_2 protons confirms the formation of N-alkylation and compound **2**. The IR spectrum of compound **3** exhibits two characteristic carbonyl peaks in the regions of 1,654 and 1,765 cm^{-1}, broad peaks at 3,365 and 3,630 cm^{-1} of the primary and secondary amine of hydrazide and 3,024 cm^{-1} for aromatic C-H group. The ^{1}H NMR spectrum of compound **3** integrates for 11 protons. A multiplet at 7.1–7.3 ppm integrates four aromatic protons, and a singlet resonates at 4.43 ppm for CH_2 protons of benzothiazinone. The absence of ester peaks and the presence of hydrazide ($NHNH_2$) protons as two singlets at 9.63 ppm and 10.30 ppm, respectively, confirm compound **3**. The IR spectrum of compounds **4a–4f** exhibits two characteristic carbonyl peaks in the regions of 1,686 and 1,731 cm^{-1}, a broad peak at 3,351 cm^{-1} N-H, at 3,039 cm^{-1} for aromatic C-H group, and a peak at 1,585 cm^{-1} for C=S. The IR spectrum of **5a** exhibits a characteristic carbonyl group peak in the region of 1,724cm^{-1}, a broad peak at 3,340 cm^{-1} for N-H, a peak at 3,024 cm^{-1} for aromatic C-H group, and a peak at 1,585 cm−1 for C=S group. The ^{1}H NMR spectrum of compound **5a** integrates for 14 protons. A multiplet at 6.53–7.55 ppm integrates for aromatic protons, a singlet at 3.41 ppm for CH_2 protons and a singlet at 4.23 ppm for CH_2 protons of benzothiazinone. A singlet peak at 13.78 ppm of NH proton of triazole (NH-C=S) confirms the formation of compound **5a**. The IR spectrum of **6a** exhibited a characteristic carbonyl group peak in the region of 1,724 cm^{-1} and at3,024 cm^{-1} for aromatic C-H group, and a peak at 1,578 cm^{-1} for the N-O group. The ^{1}H NMR spectrum of compound **6a** integrates for 17 protons. A multiplet peak at 6.91–8.03 ppm integrates for aromatic protons and protons of nitroaromatic appears as a multiplet at 8.26–8.38 ppm, a singlet at 3.41 ppm for CH_2 protons and a singlet at 4.23 ppm for CH_2 protons of benzothiazinone confirms the formation of the compound **6a**.

In-vitro antitubercular activity and CC_{50}

Synthesized benzothiazinone encompassed 3,5 disubstituted-1,2,4-triazoles (**5a–f** and **6a–d**) were tested for *in vitro* anti-TB activity against the *Mtb* strain of H37Rv. The antitubercular activity of the synthesized molecules was tested at 100–0.8 µg/ml concentrations by Microplate Alamar Blue Assay using antitubercular drugs, namely pyrazinamide, ciprofloxacin, streptomycin as the reference standard. The antitubercular activity data are depicted in Table 1. Synthesized compounds have antitubercular activity in the range of 12.5–100 µg/ml concentration. The data indicate that the compounds **5c**, **5e**, and **6c** were promising candidates during the study and demonstrated MIC at 12.5 µg/ml. Molecule **6d** has an MIC at 25 µg/ml, while **5a, 5b, 5d, 5f,** and **6a** have shown modest activity (MIC = 50 µg/ml). The compound **6b** showed the least antitubercular activity at 100 µg/ml concentration. It was observed from the data that antitubercular activity depends on substituent groups on the phenyl group at fourth position of the 1, 2, 4-triazole ring. The electron-withdrawing group (OCH_3) on phenyl group in **5c** and an electronegative atom in **5e** on phenyl ring exhibited good activity among the **5** series compounds. The substitution of 4-nitrobenzoyl group by thiol hydrogen of the **5** series did not result in better antitubercular activity. Only compound **6c** retained activity among the **6** series compounds. The CC_{50} data of the synthesized compounds against HEK293T reveal that the compounds require >132.26 µg/ml concentration to kill 50% of the viable cells. This indicates that the anti-TB activity of the synthesized molecules is not caused by the cytotoxic effect. Furthermore, it was observed that the introduction of 4-nitrobenzoyl group at the 3-thiol of triazole ring in the final compounds did not form covalent interactions with DprE1, which is evident from the molecular docking study and further exhibited CC_{50} slightly more (lower CC_{50} values) than the **5** series compounds. However, the 4-nitrobenzoyl group did not pay to the enhancement of antitubercular action.

In silico ADMET prediction

The ADMET properties of designed molecules were measured through ADMETSAR and Discovery Studio 19.0. The designed molecules showed suitable value for the evaluated *in silico* parameters (Table 2). The predicted ADMET data show that the molecules have considerable oral bioavailability and moderate acute oral toxicity. The predicted oral availability human intestinal absorption (HIA) was excellent, which displayed a calculated probability of 0.85–0.98. The predicted blood–brain barrier (BBB) penetration values suggest good penetration in the range of 0.74–0.98. The compound also exhibited moderate Caco2 cell permeability, ranging from 0.5 to 0.59 and acute oral toxicity within the range of 0.56–0.61. The literature evidence suggests that the control of lipophilicity within a particular range can increase compound features and the chance of therapeutic achievement (Arnott *et al*., 2012; Shaikh *et al*., 2016). The R in the final compounds is substituted with lipophilic modifiers to increase lipophilicity (no defilement of rule of five) values of the designed compounds and introduction of nitroaromatic functionality to realize the antitubercular potentials in additions to the final core heterocyclic moieties. The predicted clogP data (Table 2) substantiate the increase of lipophilicity of the final molecules.

Table 1. Molecular docking and *in vitro* biological activity data of structures synthesized.

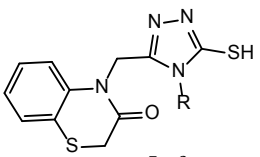

5a-f

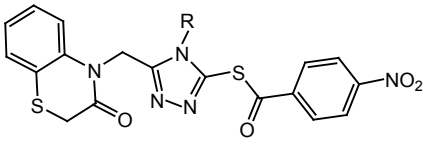

6a-d

Cpd code	R=	Molecular Docking score (Ref:4PFD)		Biological Activity (µg/ml)	
		Absolute energy (Kcal/mol)	LIBDOCK (Kcal/mol)	Mtb H37Rv (ATCC 27294)	CC_{50} (IC_{50}) HEK293T
5a	Phenyl	86.7986	113.083	50	167.41 ± 1.03
5b	Cyclohexyl	55.655	123.111	50	158.41 ± 1.27
5c	4-methoxyphenyl	98.3711	113.238	12.5	171.28 ± 1.31
5d	Naphthyl	109.113	116.292	50	169.02 ± 1.31
5e	4-fluorophenyl	77.8081	114.067	12.5	152.58 ± 1.56
5f	2-tolyl	81.2104	112.101	50	166.15 ± 1.39
6a	Phenyl	95.4647	140.368	50	149.25 ± 1.25
6b	Cyclohexyl	82.5853	139.726	100	132.26 ± 1.03
6c	4- methoxyphenyl	103.836	136.528	12.5	136.62 ± 1.03
6d	4- fluorophenyl	95.6501	136.869	25	129.73 ± 1.11
4PFD	Reference ligand	85.0753	121.706	–	–
	Streptomycin	–	–	6.25	–
	Ciprofloxacin	–	–	3.12	–
	Pyrazinamide	–	–	3.12	–
	Paclitaxel	–	–	–	0.3

Table 2. *In-silico* ADMET and clogP data of synthesized compounds.

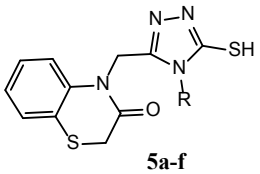

5a-f

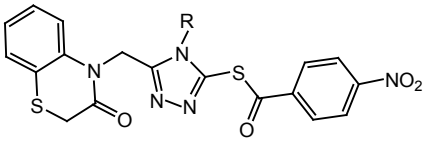

6a-d

Cpd code	BBB	HIA	Caco-2 Permeability	Acute oral toxicity	clogP
5a	0.98	0.98	0.52	0.56	3.017
5b	0.98	0.98	0.52	0.56	2.962
5c	0.98	0.99	0.5	0.56	2.99
5d	0.98	0.98	0.52	0.56	4.191
5e	0.98	0.98	0.5	0.59	3.163
5f	0.98	0.99	0.53	0.56	3.516
6a	0.85	0.95	0.58	0.61	4.023
6b	0.85	0.94	0.59	0.59	3.968
6c	0.74	0.98	0.58	0.58	4.029
6d	0.95	0.98	0.56	0.57	4.169
5[a]	–	–	–	–	1.209

[a]Not synthesized and only for prediction of clogP.

Molecular docking study

In silico prediction of ligand interactions to the target DprE1 receptor's binding site is understood through molecular docking. The application populates individual ligands' respective scores and the best conformation of different ligands (Fig. 2) to the active site. The adopted docking protocol indicates the binding affinities of designed and synthesized ligands into the binding site of the DprE1. The validation of docking was conducted by re-docking the co-crystalized ligand and evaluating the with RMSD (Root-Mean-Square Deviation) analysis. It was found that the co-crystallized ligand interacted identically to the binding site, as mentioned in the PDB. The

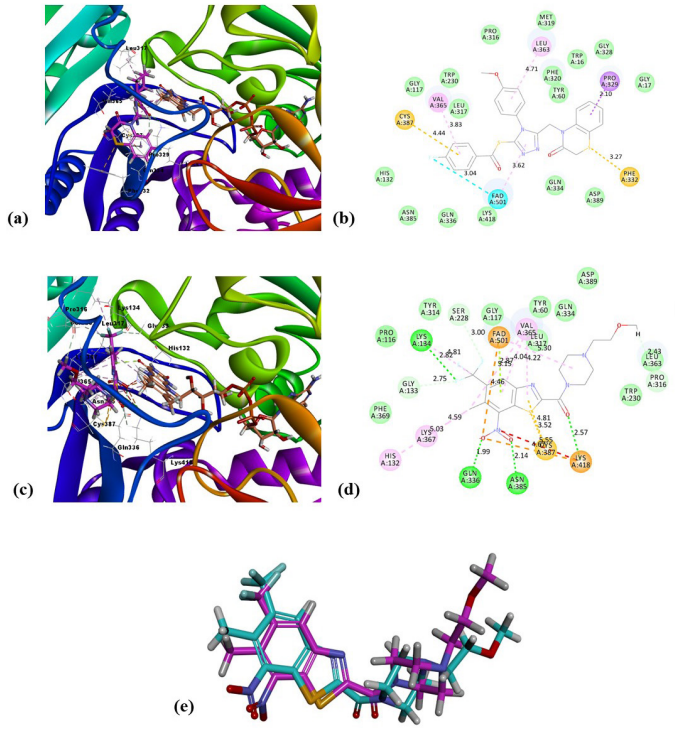

Figure 2. Docking interaction and binding mode of (**a,b**) **6c** in 3D and 2D forms at the binding site of DPrE1, (**c,d**) co-crystallized ligand in 3D and 2D forms at the binding site of DPrE1, (**e**) superposition of pre-and post-dock confirmation of co-crystalized ligand, where the cyan and purple colors represent the confirmations, respectively.

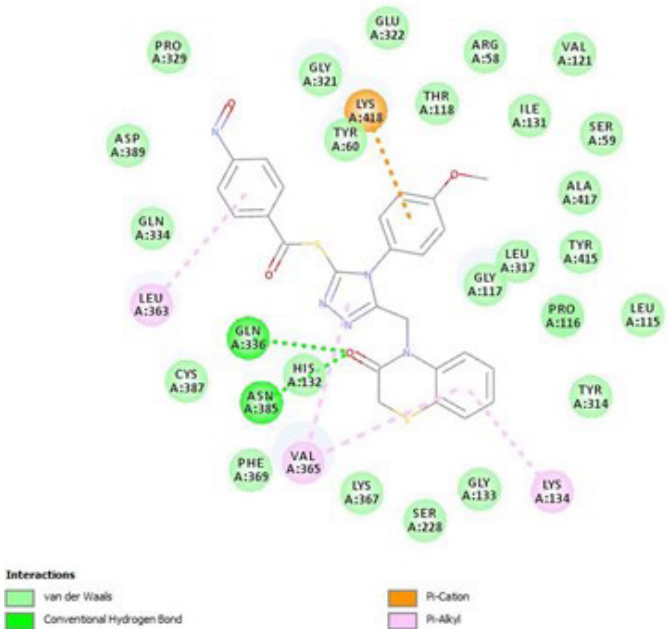

Figure 3. 2D interaction analysis of the nitroso derivative of **6c** and 4PFD.

binding affinities for respective ligands are indicated in Table 1, which indicates the individual affinities to the binding site. The compounds **6a–d** were found to be the best from the docking score. Most interacting amino acids and cofactor are LYS418, LYS134, GLN336, ASN385, PHE332, and LEU317 with FAD501, shared among all the ligands in a bound form to the DprE1 active site. Validation of docking protocol was confirmed with superimposing pre- and post-dock structures of co-crystalized ligand, having an RMSD value of 1.85 Å. Analysis of docking poses reveals the presence of hydrogen bonds and other hydrophobic interactions.

The 2D interaction analysis suggests that both compound **6c** and the non-covalent co-crystallized ligand cBT ([4-(2-methoxyethyl)piperazin-1-yl][6-methyl-7-nitro-5-(trifluoromethyl)-1, 3-benzothiazol-2-yl]methanone) forms similar π-sulfur stacking interactions between the sulfur group of CYS387 and π electrons of the phenyl ring and benzothiazole ring, respectively, at the DprE1 active site. In the known non-covalent inhibitors (BTZ 043 and PBTZ 169) of DprE1, the nitro group is present in the structure's core nucleus (benzothiazinone), while in our title compounds, the nitro group is in the side chain. Furthermore, amino acid residue CYS387 and nitro of BTZ043 is a mechanism-based covalent inhibition.

The change of the nitro group of BTZ043 to the active nitroso form requires the protein's enzymatic activity with the substrate (Piton *et al*., 2017). For further clarification, we docked our active moiety with DprE1 (4PFD) by slightly changing our compound **6c** from the nitro to nitroso group to reveal any possible interaction that may occur with nitrogen in the nitroso group and amino acid residue CYS387. The 2D interaction analysis showed (Fig. 3) that CYS387 does not form any electrostatic interaction with the nitroso group. We suggest that the title compounds may interact with a binding cavity of DprE1 in a non-covalent fashion from the above discussion. It was observed that the introduction of the nitro benzoyl moiety in the final compounds did not form covalent interactions with DprE1, hence less contributed to the overall toxicity of the final compounds. The docking protocol so adopted is in good correlation to the in vitro antitubercular activity.

CONCLUSION

New benzothiazinone linked 1,2,4-triazoles (**5a–5f, 6a–d**) were synthesized conveniently and characterized with the help of spectral studies. The *in silico* ADMET properties data provided the desired draggability of the synthesized compounds. Compounds **5c, 5e,** and **6c** were found to be active antitubercular agents among the reported derivatives. It was observed from the data that antitubercular activity depends on substituent groups on phenyl moiety at fourth position of 1, 2, 4-triazole ring. The electron-withdrawing group (OCH_3) on the phenyl group in **5c** and an electronegative atom in **5e** on the phenyl ring exhibited good activity. The substitution of the 4-nitrobenzoyl group by thiol hydrogen of the **5** series did not result in a better antitubercular activity. Only the compound **6c** retained activity among the **6** series compounds. The CC_{50} data against HEK293T reveal that the title compounds' antitubercular activity is not due to CC_{50}. The compounds **6a–d** showed good molecular docking scores, and their interactions with amino acids with active site pockets of the DprE1 are in line with the reference ligand. Hence, the study's data may provide the basis for the development of benzo[1, 4] thiazin-3(4*H*)-one encompassed 1,2,4-triazole scaffolds as potential DprE1 inhibitors.

ACKNOWLEDGMENTS

The authors are thankful to the Principal, JSS College of Pharmacy, JSS Academy of Higher Education and Research,

Mysore, India, for providing necessary facilities. The authors express their thanks to the Institution of Excellence, Vijnana Bhavan, Manasagangotri, Mysuru-570006, for spectral data. They also express their thanks to the Department of Microbiology and Molecular Biology, Maratha Mandal's NGH Institute of Dental Sciences and Research Centre, Belgaum-590 010, Karnataka, for antitubercular studies.

AUTHOR CONTRIBUTIONS

All authors made substantial contributions to conception and design, acquisition of data, or analysis and interpretation of data; took part in drafting the article or revising it critically for important intellectual content; agreed to submit to the current journal; gave final approval of the version to be published; and agree to be accountable for all aspects of the work. All the authors are eligible to be an author as per the international committee of medical journal editors (ICMJE) requirements/guidelines.

FUNDING

There is no external funding to report.

CONFLICTS OF INTEREST

The authors report no financial or any other conflicts of interest in this work.

ETHICAL APPROVALS

This study does not involve experiments on animals or human subjects.

PUBLISHER'S NOTE

This journal remains neutral with regard to jurisdictional claims in published institutional affiliation.

REFERENCES

Abrahams KA, Besra GS. Mycobacterial cell wall biosynthesis: a multifaceted antibiotic target. Parasitology, 2018; 145:116–33.

Akkerman O, Aleksa A, Alffenaar JW, Al-Marzouqi NH, Arias-Guillén M, Belilovski E, Bernal E, Boeree MJ, Borisov SE, Bruchfeld J, Loidi JC. Surveillance of adverse events in the treatment of drug-resistant tuberculosis: a global feasibility study. Int J Infect Dis, 2019; 83:72–6.

Arnott AJ, Planey LS. The influence of lipophilicity in drug discovery and design. Expert Opin Drug Discov, 2012; 7:863–75.

Bangalore PK, Vagolu SK, Bollikanda RK, Veeragoni DK, Choudante PC, Misra S, Sriram D, Sridhar B, Kantevari S. Usnic acid enaminone-coupled 1, 2, 3-triazoles as antibacterial and antitubercular agents. J Nat Prod, 2019; 83:26–35.

Batt SM, Jabeen T, Bhowruth V, Quill L, Lund PA, Eggeling L, Alderwick LJ, Fütterer K, Besra GS. Structural basis of inhibition of *Mycobacterium tuberculosis* DprE1 by benzothiazinone inhibitors. Proc Natl Acad Sci U S A, 2012; 109:11354–9.

Brecik M, Centárová I, Mukherjee R, Kolly GS, Huszár S, Bobovská A, Kilacsková E, Mokošová V, Svetlíková Z, Šarkan M, Neres J. DprE1 is a vulnerable tuberculosis drug target due to its cell wall localization. ACS Chem Biol, 2015; 10:1631–6.

Chang C, Zhu YQ, Mei JJ, Liu SQ, Luo J. Involvement of mitochondrial pathway in NCTD-induced cytotoxicity in human hepG2 cells. J Exp Clin Cancer Res, 2010; 29:145–54.

Coxon GD, Cooper CB, Gillespie SH, McHugh TD. Strategies and challenges involved in the discovery of new chemical entities during early-stage tuberculosis drug discovery. J Infect Dis, 2012; 205:S258–64.

Inturi B, Pujar GV, Purohit MN, Iyer VB, Sowmya GS, Kulkarni M. Design, synthesis and evaluation of diphenyl ether analogues as antitubercular agents. RSC Adv, 2016; 6:110571–82.

Karabanovich G, Dusek J, Savková K, Pavlis O, Pávková I, Korabecny J, Kucera T, Kočová Vlčková H, Huszár S, Konyariková Z, Konecna K. Development of 3, 5-dinitrophenyl-containing 1, 2, 4-triazoles and their trifluoromethyl analogues as highly efficient antitubercular agents inhibiting decaprenylphosphoryl-β-d-ribofuranose 2′-oxidase. J Med Chem, 2019; 62:8115–39.

Keri RS, Patil SA, Budagumpi S, Nagaraja BM. Triazole: a promising antitubercular agent. Chem Biol Drug Des, 2015; 86:410–23.

Kim P, Zhang L, Manjunatha UH, Singh R, Patel S, Jiricek J, Keller TH, Boshoff HI, Barry III CE, Dowd CS. Structu-activity relationships of antitubercular nitroimidazoles. 1. Structural features associated with aerobic and anaerobic activities of 4-and 5-nitroimidazoles. J Med Chem, 2009; 52:1317–28.

Krishna KM, Inturi B, Pujar GV, Purohit MN, Vijaykumar GS. Design, synthesis and 3D-QSAR studies of new diphenylamine containing 1, 2, 4-triazoles as potential antitubercular agents. Eur J Med Chem, 2014; 84:516–29.

Leonard B, Coronel J, Siedner M, Grandjean L, Caviedes L, Navarro P, Gilman RH, Moore DA. Inter-and intra-assay reproducibility of microplate Alamar blue assay results for isoniazid, rifampicin, ethambutol, streptomycin, ciprofloxacin, and capreomycin drug susceptibility testing of *Mycobacterium tuberculosis*. J Clin Microbiol, 2008; 46:3526–29.

Li L, Lv K, Yang Y, Sun J, Tao Z, Wang A, Wang B, Wang H, Geng Y, Liu M, Guo H. Identification of N-benzyl 3, 5-dinitrobenzamides derived from PBTZ169 as antitubercular agents. ACS Med Chem Lett, 2018; 9:741–45.

Libardo MD, Boshoff HI, Barry III CE. The present state of the tuberculosis drug development pipeline. Curr Opin Pharmacol, 2018; 42:81–94.

Maddila S, Pagadala R, Jonnalagadda SB. 1, 2, 4-triazoles: a review of synthetic approaches and the biological activity. Lett Org Chem, 2013; 10:693–714.

Magnet S, Hartkoorn RC, Székely R, Pató J, Triccas JA, Schneider P, Szántai-Kis C, Őrfi L, Chambon M, Banfi D, Bueno M. Leads for antitubercular compounds from kinase inhibitor library screens. Tuberculosis, 2010; 90:354–60.

Makarov V, Manina G, Mikusova K, Möllmann U, Ryabova O, Saint-Joanis B, Dhar N, Pasca MR, Buroni S, Lucarelli AP, Milano A. Benzothiazinones kill *Mycobacterium tuberculosis* by blocking arabinan synthesis. Science, 2009; 324:801–4.

Makarov V, Neres J, Hartkoorn RC, Ryabova OB, Kazakova E, Šarkan M, Huszár S, Piton J, Kolly GS, Vocat A, Conroy TM. The 8-pyrrole-benzothiazinones are non-covalent inhibitors of DprE1 from *Mycobacterium tuberculosis*. Antimicrob Agents Chemother, 2015; 59:4446–52.

Manina G, Bellinzoni M, Pasca MR, Neres J, Milano A, de Jesus Lopes Ribeiro AL, Buroni S, Škovierová H, Dianišková P, Mikušová K, Marák J. Biological and structural characterization of the mycobacterium smegmatis nitroreductase NfnB, and its role in benzothiazinone resistance. Mol Microbiol, 2010; 77:1172–85.

Naik M, Humnabadkar V, Tantry SJ, Panda M, Narayan A, Guptha S, Panduga V, Manjrekar P, Jena LK, Koushik K, Shanbhag G. 4-aminoquinolone piperidine amides: non-covalent inhibitors of DprE1 with long residence time and potent antimycobacterial activity. J Med Chem, 2014; 57(12):5419–34.

Neenu G, Arun KS, Manisha S, Chandrashekar VM, Pujar GV. Antitubercular potential of novel isoxazole encompassed 1, 2, 4-triazoles: design, synthesis, molecular docking study and evaluation of antitubercular activity. Antiinfect Agents, 2020; 18. https://doi.org/10.2174/2211352518999200711163714

Piton J, Foo CS, Cole ST. Structural studies of *Mycobacterium tuberculosis* DprE1 interacting with its inhibitors. Drug Discov Today, 2017; 22:526–33.

Prasad R, Singh A, Balasubramanian V, Gupta N. Extensively drug-resistant tuberculosis in India: current evidence on diagnosis & management. Indian J Med Res, 2017; 145:271–93.

Rabie R, Hammouda MM, Elattar KM. Cesium carbonate as a mediated inorganic base in some organic transformations. Res Chem Intermed, 2017; 43:1979–2015.

Rajender O, Narsimha S, Reddy VN. Design, synthesis and *in vitro* anticancer evaluation of new 2H-benzo[b][1,4]thiazin-3(4H)-one based 1,2,3-triazoles. Asian J Chem, 2019; 31(11):2647–52.

Reddyrajula R, Dalimba U. The bioisosteric modification of pyrazinamide derivatives led to potent antitubercular agents: synthesis via click approach and molecular docking of pyrazine-1, 2, 3-triazoles. Bioorg Med Chem Lett, 2020; 30:126846.

Rojano B, Caminero JA, Hayek M. Curving tuberculosis: current trends and future needs. Ann Glob Health, 2019; 85:1–7

Shaikh MH, Subhedar DD, Arkile M, Khedkar VM, Jadhav N, Sarkar D, Shingate BB. Synthesis and bioactivity of novel triazole incorporated benzothiazinone derivatives as antitubercular and antioxidant agesnt. Bioorg Med Chem Lett, 2016; 15;26:561–69.

Shaikh MH, Subhedar DD, Nawale L, Sarkar D, Khan FA, Sangshetti JN, Shingate BB. Novel benzylidenehydrazide-1, 2, 3-triazole conjugates as antitubercular agents: synthesis and molecular docking. Mini Rev Med Chem, 2019; 19:1178–94.

Shirude PS, Shandil R, Sadler C, Naik M, Hosagrahara V, Hameed S, Shinde V, Bathula C, Humnabadkar V, Kumar N, Reddy J. Azaindoles: non-covalent DprE1 inhibitors from scaffold morphing efforts, kill *Mycobacterium tuberculosis* and are efficacious *in vivo*. J Med Chem, 2013; 56:9701–08.

Tiwari R, Miller PA, Chiarelli LR, Mori G, Šarkan M, Centárová I, Cho S, Mikušová K, Franzblau SG, Oliver AG, Miller MJ. Design, syntheses, and antitubercular activity of 1, 3-benzothiazinone azide and click chemistry products inspired by BTZ043. ACS Med Chem Lett, 2016; 7:266–70.

Wang F, Sambandan D, Halder R, Wang J, Batt SM, Weinrick B, Ahmad I, Yang P, Zhang Y, Kim J, Hassani M. Identification of a small molecule with activity against drug-resistant and persistent tuberculosis. Proc Natl Acad Sci USA, 2013; 110:E2510–17.

Wolucka BA, McNeil MR, de Hoffmann E, Chojnacki T, Brennan PJ. Recognition of the lipid intermediate for arabinogalactan/arabinomannan biosynthesis and its relation to the mode of action of ethambutol on mycobacteria. J Biol Chem, 1994; 269:23328–35.

Zampieri D, Cateni F, Moneghini M, Zacchigna M, Laurini E, Marson D, De Logu A, Sanna A, Mamolo MG. Imidazole and 1, 2, 4-triazole-based derivatives gifted with antitubercular activity: cytotoxicity and computational assessment. Curr Top Med Chem, 2019; 19:620–32.

Zhang L, Peng XM, Damu GL, Geng RX, Zhou CH. Comprehensive review in current developments of imidazole-based medicinal chemistry. Med Res Rev, 2014; 34:340-437.

How to cite this article:
Ajmal K, Pujar GV, Kumar SA, Mandal SP, Singh M. New benzothiazinone linked 1, 2, 4-triazoles: Design, synthesis, characterization, and evaluation of antitubercular activity. J Appl Pharm Sci, 2021; 11(02):029–038.